

FRAS: Federated Reinforcement Learning empowered Adaptive Point Cloud Video Streaming

Yu Gao, Zhi Liu, Bo Han, Pan Hui, Pengyuan Zhou*

ABSTRACT

Point cloud video transmission is challenging due to high encoding/decoding complexity, high video bitrate, and low latency requirement. Consequently, conventional adaptive streaming methodologies often find themselves unsatisfactory to meet the requirements in threefold: 1) current algorithms reuse existing quality of experience (QoE) definitions while overlooking the unique features of point cloud video thus failing to provide optimal user experience, 2) most deep learning approaches require long-span data collections to learn sufficiently varied network conditions and result in long training period and capacity occupation, 3) cloud training approaches pose privacy risks caused by leakage of user reported service usage and networking conditions.

To overcome the limitations, we present FRAS, the first federated reinforcement learning framework, to the best of our knowledge, for adaptive point cloud video streaming. We define a new QoE model which takes the unique features of point cloud video into account. Each client uses reinforcement learning (RL) to train encoding rate selection with the objective of optimizing the user's QoE under multiple constraints. Then, a federated learning framework is integrated with the RL algorithm to enhance training performance with privacy preservation. Extensive simulations using real point cloud videos and network traces reveal the superiority of the proposed scheme over baseline schemes. We also implement a prototype that demonstrates the performance of FRAS via real-world tests.

1 INTRODUCTION

Volumetric video becomes a research hotspot in recent years thanks to its immersive viewing experience with six degrees of freedom, i.e., 6DoF, including the position (X, Y, Z) and the orientation (yaw, pitch, roll) of the viewer. Users can freely select any preferred viewing angle of the 3D scene to get experience beyond 360-degree video which is restricted to 3DoF. In other words, unlike 3DoF 360-degree video systems in which users can only switch orientation, in a volumetric video user can freely move body position besides head direction to subscribe to a field of view (FoV) at any location within the scene.

Point cloud is arguably the most promising volumetric video format and has drawn great attention from both

academia and industry [2, 18, 22]. Delivering point cloud video requires transmission-friendly encoding, bandwidth-aware quality level adaption, efficient quality assessment metrics, and accurate 6DoF motion prediction [5, 21]. For instance, the required bandwidth for a point cloud video streaming at 30 frame per second can be as high as 6 Gbps [6] due to the large sizes of raw point cloud frames, demanding efficient transmission methods.

Encoding/compression hence has been widely explored to guarantee transmission efficiency and user experience [3, 22]. Tiling is popularly adopted as well since a user can watch only a portion of the scene at a time [13, 20]. For example, Park et al. proposed to partition the point cloud video into tiles spatially. Each tile is encoded into different quality levels depending on its relation to the user's view frustum and distance to the user [20]. However, the decoding of point cloud video requires more computation than traditional video [13, 15, 24], posing a distinguished challenge for point cloud video systems. A few works consider uncompressed tiles to relieve the burden of en(de)coding. For example, Li et al. considered the uncompressed tiles and optimize the user's quality of experience (QoE) by selecting the proper quality levels under the communication and computation constraints [13]. Liu et al. proposed a fuzzy logic solution to select the quality level for each tile based on the future bandwidth, user FoV, and the available computation capability [14]. However, these schemes require predefined models or rules and thus cannot adapt to the dynamic network conditions. Although there are adaptive streaming approaches for traditional video streaming, such proposal for point cloud streaming is yet to be explored.

To this end, this paper provides a federated reinforcement learning (RL) empowered point cloud video streaming system, FRAS. The point cloud video is properly partitioned into tiles with different quality levels and different computation requirements for decoding. A novel quality evaluation metric for point cloud videos is proposed thereafter, which takes into account of the point cloud video system features such as decoding complexity and viewer position. Then based on the predicted network bandwidth and viewing direction and the decoding complexity, RL empowered quality level selection helps maximize the perceived user experience under the constraints of communication resources, computation resource, and user quality requirements. To augment the

*Corresponding author: Pengyuan Zhou, E-mail: (pyzhou@ustc.edu.cn).

training performance restricted by local datasets, FRAS applies federated learning to aggregate the learning experience of distributed clients while protecting their privacy. Extensive simulations based on real point cloud video sequences and network traces are conducted and the results reveal the superiority of the proposed scheme over baseline schemes including QUETRA [28], Pensieve [16], robustMPC [30], and Buffer-Based (BB) [11]. To the best of our knowledge, this is the first paper studying point cloud video streaming using federated RL. Our contributions are summarized as follows:

- We propose FRAS, a federated reinforcement learning empowered adaptive point cloud streaming framework. FRAS leverages distributed clients' datasets to improve the learning performance with privacy preservation. FRAS is the first federated learning based adaptive streaming (not only point cloud video but in general) to our best knowledge.
- We propose a novel QoE definition which takes unique features of point cloud video into account.
- Extensive simulations based on real point cloud video sequences and network traces are conducted and the results reveal the superiority of the proposed scheme over baseline schemes. FRAS outperforms SOTA methods by up to 86%, 77%, 12%, and 75% on the performances of QoE, quality level, PSNR, and rebuffering, respectively. We implement a prototype of FRAS and validates its performance via real-world tests.

2 BACKGROUND

Point cloud encoding and processing. Point cloud is composed of points represented in the 3D space, each point is associated with multiple attributes such as coordinate and color. There are two major classes of point cloud encoding methods according to point cloud data distribution [3, 22]. Point cloud with uniform distribution can be projected into 2D frames using well-known 2D video technologies while sparse distributed point cloud data can be decomposed into hierarchical cubes with each point encoded as an index of its belonging cube. Note that the point cloud encoding has higher computation complexity than the traditional video [13, 21].

Point cloud quality assessment defines the optimization objective and is an essential component of the point cloud video transmission system. Traditional video transmission commonly uses peak signal-to-noise ratio (PSNR), which calculates the pixel-to-pixel difference between the ground truth frame and the relieved frame, for quality assessment. For point cloud video quality assessment, researchers have proposed several metrics with similar logic. For example, [9] uses the PSNR of point-to-point distortions to measure the objective quality with the MPEG PCC quality metric software. [20] introduces utility measures based on the underlying

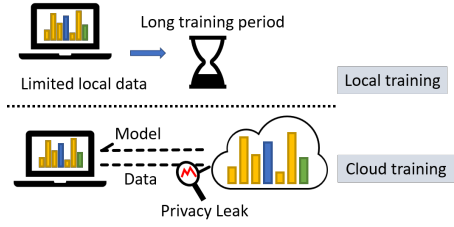


Figure 1: Shortcomings in existing approaches.

quality of the representation, the level of details to the user's viewpoint and device resolution. However, these schemes basically inherit the traditional video metrics and do not fully take the features of point cloud video into account.

Point cloud video streaming has drawn more and more attentions recently [5, 13]. Most of these works use similar methods with VR video streaming method [8, 31] that divide the videos into smaller tiles and only transmit the tiles inside user's FoV with the goal of optimizing the defined objective function [20, 24]. [13] considers the high computation complexity of point cloud video encoding during transmission optimization. These schemes are model based and not adaptive to the dynamic network conditions.

RL has become popular in traditional video streaming in recent few years [16, 27]. M. Claeys, et al. [4] designed a RL-based HTTP adaptive streaming client that is capable of dynamical adaption by interacting with the environment to optimize the QoE. The challenges in this direction include the proper definition of the reward and the training algorithm. Moreover, conventional local training provokes a significant limitation on the scale of training dataset, specifically constrained to individual user devices. Since the networking condition varies from session to session, each device needs a long-span data collection and training period to learn different networking conditions. As pointed out by Pensieve [16], retraining frequency depends on the generalizability of the model and the frequency of new network behaviors. The authors in Oboe [1] further demonstrate the necessity of retraining for Pensieve in the face of different network conditions. Furthermore, collecting distributed users' datasets and train a global model in a cloud datacenter poses privacy risk and concern for the users.

To address the aforementioned shortcomings of related approaches as depicted in Figure 1, we propose FRAS, a cross-device federated reinforcement learning adaptive streaming system to augment local model training via aggregation the learning experience from distributed clients. FRAS takes the decoding complexity and features of point cloud into the account of learning policy. Moreover, unlike current schemes relying on local user data [16, 29], FRAS leverages uniquely

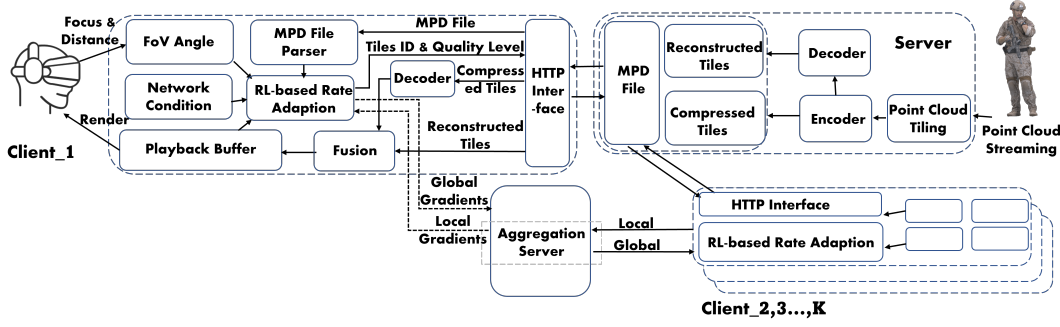


Figure 2: FRAS system architecture

diverse datasets from distributed users via federated learning to explore the generalizability of models extracting from global learning experience. Without requiring user data uploading, FRAS guarantees privacy and non-identifiability for the resulting models [12].

3 FRAS SYSTEM

This section introduces the tiling and quality assessment metric of point cloud videos.

3.1 System overview

As illustrated in Figure 2, the point cloud video cameras capture the target scene from different angles simultaneously. The video is delivered to the server through wired network and then tiled. Then the sever generates a MPD file using the encoded tiles and reconstructed tiles and sends it to the clients. Then each client uses the RL-based rate adaption to select tiles ID and quality level based on environment information such as FoV angle, network condition, buffer state, and tiles information obtained from the MPD file. Thereafter, the clients get required tiles through HTTP interface. Meanwhile, multiple clients aggregate gradients via the aggregation server through FRAS algorithm during the training phase.

Since the bandwidth between video source and server is normally sufficient, we focus on the transmission between server and client which has limited and dynamic bandwidth $B_{i,t}$ for client i at time point t . Note that t is the basic time unit during which the frames are encoded together as a group, similarly as the group of pictures (GoP) in traditional video streaming. $B_{i,t}$ is predicted by employed bandwidth prediction methodology as explained in Section 3.3. Consider client i has a FoV $F_{i,t}$ at time point t demanding video quality not lower than Q_i . User i has $C_{i,t}$ available computation capacity to decode the compressed tiles. The client makes the decisions using RL based on the viewing angle, bandwidth, playback buffer and the decoding process complexity according to the predefined reward policy to optimize QoE.

3.2 Tiling

To guarantee the smooth viewing angle switch and high video quality within the client's FoV, the point cloud video is partitioned into tiles and only the tiles within the client's FoV are transmitted for efficient bandwidth usage. First, we recognize the best-fit cuboid surrounding the interested point cloud space and identify its pose and 3D dimension. Then, we perform $N \times M$ partitioning on the plane perpendicular to the height and dividing them into H layers in the height direction, and finally, $N \times M \times H$ tiles are obtained as shown in 3. The partitioned tiles at t are compressed into L quality levels. A tile $\{(n, m, h, t) | 1 \leq n \leq N, 1 \leq m \leq M, 1 \leq h \leq H\}$ encoded at quality level l ($1 \leq l \leq L$) has data size of $s_{n,m,h,l,t}$, point-to-point PSNR $q_{n,m,h,l,t}$, and computational requirement $d_{n,m,h,l,t}$ for decoding. Higher quality level results in larger source encoding size.

We consider that the server also decodes each compressed tile and thus has uncompressed tiles at all quality levels. An uncompressed tile (n, m, h, t) with quality level l ($1 \leq l \leq L$) is with source encoding size $s'_{n,m,h,l,t}$, point-to-point PSNR $q_{n,m,h,l,t}$, and do not require computational capacity for decoding. We consider lossless compression in this work to avoid lossy compression's impact on depth data [25] and thus the uncompressed tiles have same PSNR values with the compressed ones encoded at the same quality levels. The uncompressed tiles are with larger rate, i.e., $s'_{n,m,h,l,t} > s_{n,m,h,l,t}$. By preparing the uncompressed tiles, we can reduce the decoding workload on the client devices with the cost of more bandwidth.

3.3 FoV and Network Prediction

FoV is determined mainly by two factors, namely, viewer position (distance to the scene) and viewer direction (which area to look at). The two factors can be learned by head and body motion prediction method, which is well explored and mature in VR video streaming [10] and can be applied for point cloud video streaming. Since this paper focuses on the

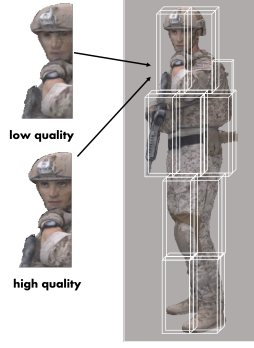


Figure 3: Tiling and encoding qualities.

adaptive streaming, we skip details of such predictions and assume the viewing position and direction are known.

Inspired by [7], we use the gated recurrent unit (GRU) for the future bandwidth prediction as shown in Figure 4. GRU is a popular artificial recurrent neural network architecture widely used for time-series data. It is similar with long short-term memory (LSTM) but with a forget gate, and can achieve slightly better performance with much lower complexity in comparison with LSTM.

3.4 Constraints

We first define two notations to facilitate the description of the quality level selection. $I_{n,m,h,l,t}$ denotes the compressed tile (n, m, h) at quality level l during time period t , where $I \in \{0, 1\}$ represents the decision of transmission, 1 transmitted and 0 otherwise. Similarly, $I'_{n,m,h,l,t}$ denotes the uncompressed tile (n, m, h) at quality level l during t . We briefly list the constraints as follows.

$$\sum_{l=1}^{l=L} I_{n,m,h,l,t} + I'_{n,m,h,l,t} = 1, \forall n, m, h, t \quad (1)$$

$$\sum_{n=1}^{n=N} \sum_{m=1}^{m=M} \sum_{h=1}^{h=H} \sum_{l=1}^{l=L} I_{n,m,h,l,t} \times s_{n,m,h,l,t} + I'_{n,m,h,l,t} \times s'_{n,m,h,l,t} \leq B_{i,t} \quad (2)$$

$$\sum_{n=1}^{n=N} \sum_{m=1}^{m=M} \sum_{h=1}^{h=H} \sum_{l=1}^{l=L} I_{n,m,h,l,t} \times d_{n,m,h,l,t} \leq C_{i,t} \quad (3)$$

which refer to the constraints of quality level selection, communication resource, and computation capacity for decoding, respectively. The constraints are quite simple and straightforward and thus we skip the detailed descriptions due to space limit.

4 FRL EMPOWERED TRANSMISSION

4.1 Challenges

This section introduces the adopted federated reinforcement learning (FRL) for adaptively selecting the proper tile quality

level to maximize QoE under the communication and computation constraints. As the first look into this problem, we summarize the challenges as follows.

- (1) The decoding complexity is a unique feature of point cloud video compared to conventional video. We need to convert it to be comparable with other metrics to integrate it into QoE calculation.
- (2) Another unique feature of point cloud video, 6DoF, enables clients to move positions. As a client would expect different frame qualities from different distances, the distance to the scene should also be considered.
- (3) Each round of federated learning consists of a number of local training epochs followed by the aggregation of clients' model updates. Therefore, a proper number of local training epochs is critical as too many would result in slow global model convergence while too few would lead to slow local model convergence and high communication cost.
- (4) Lastly, though network prediction is not the focus of this work, it is an interesting additional functionality to improve ABR in general. Hence, it is important to ensure its processing delay does not impact the streaming service.

4.2 QoE Definition

We mainly consider the point-to-point PSNR, encoding quality level, and the distance from the scene for the quality metric. When a client moves closer to the scene, the number of tiles within the FoV decreases, and we assume each tile's PSNR tends to be more important, and vice versa. Furthermore, the client would expect a clearer scene when moves closer, which also backs up our assumption. Thus, for each client i with FoV $F_{i,t}$ at time t , the quality of its received video is defined as follows:

$$Q = \alpha * \sum_{FoV} q_{n,m,h,l,t} / dis + \beta * l \quad (4)$$

which indicates the weighted sum of the encoding quality level and the summed point-to-point PSNR value of the tiles within the FoV considering the inverse correlation with the distance. Next, the optimization goal also considers the rebuffering time T_r and quality smoothness Δl as in other related works. Moreover, as mentioned before, we take the decoding complexity of point cloud video into account. Since QoE already contains quality metrics and time metrics, adding a third-dimension metric would further increase its complexity and the training difficulty. Hence, instead of directly using required decoding capacity, we include decoding time T_d in the QoE. We conducted numerous decoding tests across different point cloud videos on varied qualities and used the average values in the algorithm. Notably, the decoding time of point cloud video tile is much larger than

that of conventional video which normally is considered an instantaneously part within T_r , as proved by our decoding tests. As such, the QoE of point cloud video streaming can be formulated as follows.

$$QoE = f(Q, T_r, \Delta l, T_d) \quad (5)$$

$$= \alpha * \sum_{FoV} q_{n,m,h,l,t} / dis + \beta * l + \gamma * T_r + \delta * \Delta l + \epsilon * T_d$$

where $\alpha, \beta, \gamma, \delta$, and ϵ are weight parameters. The problem is to maximize the average QoE. As such, we solve **challenge 1 and 2**.

4.3 FRL Algorithms

We conduct local training with RL algorithm for optimizing each individual clients' QoE following the objective function defined in Section 4.2. As mentioned, each client encounters limited networking conditions in short periods and thus needs a long-span data collection and training to get a generalized and robust model, which impacts the QoE of client and battery life of device. Therefore, we integrate FL and RL to aggregate the learning experience across users for data augmentation and training acceleration under privacy preservation. The major details are listed as follows.

State: The RL agent takes $s_t = (l_{t-1}, b_t, B_t, d_t, n_t, r_t)$ as the input, where l_{t-1} is the selected encoding quality level of the last point cloud video chunk (uncompressed tiles have different level indices than compressed tiles to differentiate); b_t is the current buffer level; B_t is the predicted network bandwidth; d_t is the download time of the current chunk; n_t is a vector of L possible sizes for the next video chunk; r_t is the number of remained chunks in the video.

Action: The RL agent takes an action by selecting the encoding quality level for the next point cloud video chunk upon receiving s_t . The actions are selected based on a policy $\pi_\theta : \pi_\theta(s_t, a_t) \rightarrow [0, 1]$

Local training: We employ actor-critic algorithm to train the local policy. The reward is defined according to QoE (Section 4.2) as shown in Equation (6). The gradient of the cumulative discounted reward with respect to the policy is computed as Equation (7) [19].

$$r_t = QoE \quad (6)$$

$$\nabla_\theta \mathbb{E}_{\pi_\theta} \left[\sum_{t=0}^{\infty} \gamma^t r_t \right] = \mathbb{E}_{\pi_\theta} [\nabla_\theta \log \pi_\theta(s, a) A^{\pi_\theta}(s, a)] \quad (7)$$

Global aggregation: We apply FedAvg[17] in the global aggregation stage. After E local epochs, m of K clients return their local gradients to the aggregation server, where m equals to $\max(\mu * K, 1)$ and μ is a pre-defined participation ratio. Then the global gradients are calculated according to

Algorithm 1: FRAS

```

1 Procedure FL:
   Input: Server weight  $\theta_0^G$ , users  $\langle c_1, c_2, \dots, c_K \rangle$ ,
   local update step  $E$ 
2 for  $T = 1$  to  $T_{max}$  do
3   Select a number of users  $C = \langle C_1^T, \dots, C_{CK}^T \rangle$ ;
4    $u_{T+1}^C \leftarrow RL(\theta_T^G)$ ;
5    $u_{T+1}^G \leftarrow FedAvg(u_{T+1}^C)$ ;
6   Update global model  $\theta_{T+1}^G \leftarrow \theta_T^G + u_{T+1}^G$ ;
7 Procedure RL:
   Input:  $C = \langle C_1^t, \dots, C_{CK}^t \rangle$ , global model  $\theta_T^G$ 
8 for each user  $c \in C$  do
9   Reset  $d\theta$  and  $d\theta_v$  to 0,  $\theta \leftarrow \theta_T^G$ ;
10   $\theta' = \theta$ ,  $\theta'_v = \theta_v$ ;
11  for  $t = t_{start}$  to  $t_{start+E-1}$  do
12     $FoV_t, B_t = Prediction(c)$ ;
13     $n_t \leftarrow f(FoV_t)$ ;
14     $s_t = (l_{t-1}, b_t, B_t, d_t, n_t, r_t)$ ;
15    Perform  $a_t$  according to  $\pi(a_t|s_t; \theta')$ ;
16    Receive reward  $r_t$  and new state  $s_{t+1}$ 
17  for  $t \in \{t_{start+E-1}, \dots, t_{start}\}$  do
18     $d\theta \leftarrow$ 
19       $d\theta + \nabla_{\theta'} \log(\pi(a_t|s_t; \theta')(R - V(s_t; \theta'_v)))$ ;
20     $d\theta_v \leftarrow d\theta_v + \frac{\partial((R - V(s_t; \theta'_v))^2)}{\partial \theta'_v}$ ;
21   $t_{start} \leftarrow t_{start+E}$ ;
22  Update  $\theta$  and  $\theta_v$ ;
23  Return  $d\theta$ 
24 Procedure Prediction:
25    $FoV \leftarrow FoVpredict(c)$ ;
26    $B \leftarrow BWpredict(c)$ ;
   Return  $c_{FoV}, c_B$ ;

```

Equation (8) and used by all the K clients to update local models.

$$\theta_t^G = \sum_{k=1}^{\mu * K} \frac{w_k * \theta_t^k}{\mu * K} \quad (8)$$

where θ_t^G and θ_t^k indicate the global and local gradients, w_k is the weight of client k .

Algorithm 1 summarizes the overall functionalities. In detail, before each round the server selects a ratio of the clients to participate the training. Each selected client trains a local actor-critic model using its own dataset. Before each training step, the client predicts the FoV and bandwidth using the methods described in Section 3.3. The client uses the predicted FoV and possible encoding quality levels to calculate the possible sizes of the next video chunk. As such, each client collects the current state s , performs action according

to the policy π , and accumulates the reward. Using the forward view and mix of n -step returns methods of actor-critic algorithm, each client accumulates the gradients of its policy and value-function. Every E epochs, the policy and value-function are updated and the policy gradients are uploaded to the server for aggregation. Upon receiving sufficient updates, the server conducts FedAvg over the gradients and updates the global model. Then the server sends the global model to another batch of selected clients and starts the next round of training until the global model converges.

Note that the integration of FL and RL is not straightforward and does require some fine-tuning efforts. As stated in **challenge 3**, the E local epochs of RL training affects the trade-off between transmission cost and convergence rate of local and global models. We found the optimal E for different data distributions via empirical tests. For **challenge 4**, to enable real-time network prediction, we customize the input/output period lengths to decrease the processing delay to a level that can be transparent to the user while still facilitating RL training and inference. Please refer to Section 5 for the details. Another ad-hoc configuration is the number of workers ran by each client’s RL algorithm. Depending on the available capacity, each RL algorithm can run varied numbers of workers on parallel using asynchronous actor-critic algorithm (A3C [19]), or, just one single worker using synchronous update (A2C [26]). The performance of both methods are comparable as found by empirical study [26]. A few newer RL algorithms can also be applied in this context which is not our focus and thus left out of this work.

5 EVALUATION

5.1 Experimental Setup

Video source. We use 36 point cloud video sequences from Panoptic Studio¹ for training. We use another 6 point cloud video sequences from vsenseVVDB2 database², i.e., *AxeGuy*, *LubnaFriends*, *Rafa2*, *Matis*, *Loot* and *Longdress*, for testing. Each point cloud video is partitioned into $3 \times 3 \times 4$ tiles and encoded by the VPCC-TMC-v7 codec³ at (geometryQP, textureQP) in $\{(32, 42), (28, 37), (24, 32), (20, 27), (16, 22)\}$.

Network conditions. To emulate realistic throughput fluctuations, we replay the bandwidth traces from a broadband dataset provided by the FCC and a 4G/LTE dataset captured during mobility [23] to simulate the network. The dataset contains 40 logs with different scenarios: foot, bicycle, bus, tram, train and car, covering 5 hours of active monitoring. Since some traces have extremely high bandwidth, we scale the traces linearly to emulate difference network conditions.

¹<http://domedb.perception.cs.cmu.edu/ptcloudodb.html>

²<https://v-sense.scss.tcd.ie/research/6DoF/quality-assessment-for-fvv-compression/>

³<https://github.com/MPEGGroup/mpeg-pcc-tmc2>

The average bandwidth is 15 Mb after scaled. During the test, the algorithm uses predicted bandwidth as described in Section 3.3 to select the encoding quality for the next video chunk. Then the algorithm uses the selected quality level and replayed bandwidth together with several other state metrics to calculate the reward.

FoV. As mentioned in Section 3.3, there are head and body motion prediction methods applicable for FoV prediction in this context. Since it is not the focus of this work, we replace it with a simple yet effective configuration. For viewer’s distance to the scene, which determines the number of tiles within the FoV, we employed a random distribution. The viewer has 50% of chance to move and 50% remain the position. Upon moving, the moving distance is selected randomly within a step length. As such, we got dynamic distance traces. For viewer direction, we found via statistical study that it has negligible affect on the data volume of the FoVs containing same number of tiles (determined by distance) at different parts of the scene. Hence, it is not important in regards of training the streaming algorithm. However, to make the test more realistic and observe the performance in visionary implementation, we deployed a straightforward yet reasonable logic that the client’s gaze moves to a farther tile with lower probability. Specifically, we took the center of current FoV as the root tile and used its radius to index the surrounding tiles. That is, the longer radius exists between a tile and the root, the larger index it has. Then we assumed all the tiles followed a Zipf distribution in terms of their ratio to be the center of next FoV. As such, we got the viewer direction traces. Under the assumption that users can move position and switch viewing direction at each frame boundary, we updated FoVs between every two frames.

Models and Metrics. FRAS passes 12 past bandwidth measurements to a 1D convolution layer with 128 filters, each of size 4 with stride 1. Possible next chunk sizes are input to another 1D-CNN with the same shape. Results from these layers are then aggregated in a 128-neuron hidden layer to apply the softmax function. The critic network uses the same structure but a linear neuron as the final output. We set the discount factor $\gamma = 0.99$, the learning rates at 10^{-4} and 10^{-3} for the actor and critic, and, the entropy factor β decay from 5 to 0.1 over 3×10^5 iterations. We implemented this architecture using TensorFlow.

Baselines. We implement 4 baselines for performance comparison. (1) QUETRA [28] is a DASH rate adaptation algorithm which calculates the expected buffer occupancy using selected bitrate, network throughput, and buffer capacity based on queuing model. (2) An RL method adapted from Pensieve [16] which trains a single RL model. (3) robustMPC [30]

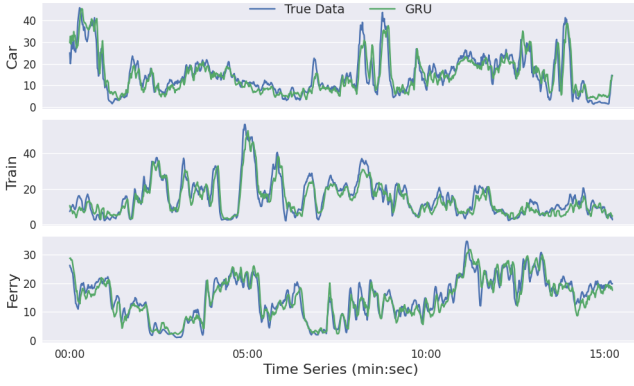


Figure 4: Network prediction in different conditions. Y axis indicates bandwidth in Mbps.

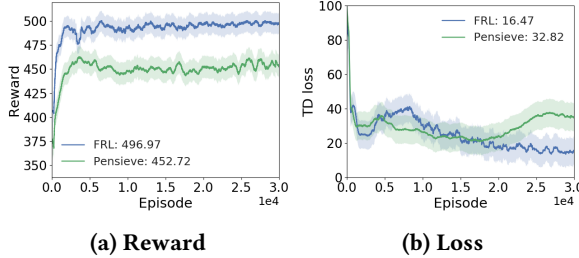


Figure 5: Comparison of FRL and Pensieve in training.

improves MPC by accounting for errors of predicted throughput via normalization. (4) Buffer-Based (BB) [11] selects the encoding quality level based on the current buffer occupancy and estimated occupancy during startup phase with the goal of keeping the occupancy above 0.1 second, and automatically chooses the highest level if the occupancy exceeds 1 second.

Implementation. We built a point cloud visualizer using PCL 1.9.1 and QT 5.12 to support each of the aforementioned baselines. The visualizer was configured to fetch quality selection decisions from an ABR client that implemented the corresponding algorithm. The player was configured to have a playback buffer capacity of 500 ms. Additionally, each video was divided into 300 chunks and had a total length of 10 seconds. Thus, each chunk represented approximately 33 ms of video playback. The video player and the ABR server ran on the same server as the client, which is equipped with Intel Xeon Gold 6246R CPU, NVIDIA GeForce GTX 3090 GPU and 480G SSD. And a HTTP server was deployed with Python HTTP module, which stored tiled point cloud videos and corresponding MPD files.

5.2 Result and Analysis

Network prediction. First, FRAS uses GRU-based method as mentioned in Section 3.3 to predict the network bandwidth

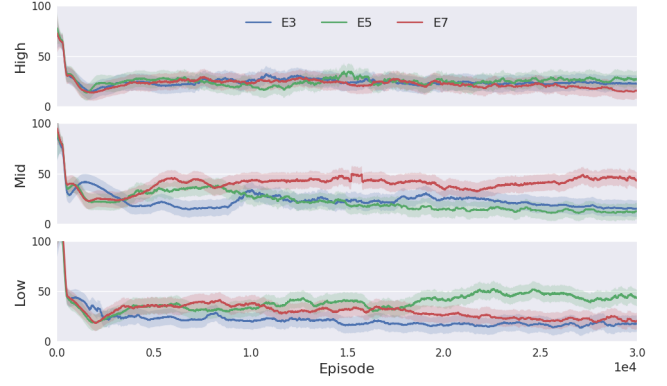


Figure 6: Effect of E in different data distribution heterogeneities. Y axis indicates loss.

for better learning performance. Figure 4 shows 3 representative networking conditions, namely, network conditions in car, tram, and ferry. As shown, the algorithm can predict the future bandwidth fairly well in varied scenarios. Specifically, we let the algorithm learn the bandwidth of the last 30 seconds and predict the next second, which takes 0.2 s on average. In other words, we can let RL learn and infer the next action in advance by 0.8 s.

Training. We first validate the core algorithm FRL by comparing its training performance with the RL algorithm adapted from Pensieve. Figure 5a and Figure 5b show the reward and loss of both algorithms during training. The curves of FRL represent the corresponding values of the global FL model while the curves of RL represent the corresponding values of an individual client model. The converged FRL outperforms Pensieve on reward by 9.77% and loss by 49.81%.

As mentioned in Section 4, the number of local RL epochs, E , before each FL aggregation affects the performance trade-off. We varied the data distribution heterogeneity across the clients and observed a pattern between the heterogeneity and optimal E value. As shown in Figure 6, as the heterogeneity increases, the algorithm requires a larger E for good performance, which is reasonable since heterogeneous data distribution demands more local training to favor each individual dataset's pattern.

Test. We validate the performance of FRL in comparison with the baselines using bandwidth traces collected in different networking conditions. As shown in Figure 7, FRL significantly outperforms the baselines in all metrics under most scenarios. Specifically, FRL increases the average QoE (reward) by 86%, 38%, 26%, and 28% compared to QUETRA, Pensieve, robustMPC, and BB, respectively. Moreover, FRL increases the average encoding quality level by 24%, 24%, 77%, and 38%, average PSNR by 3%, 3%, 12%, and 8%, average rebuffer time by 50%, 66%, 50%, and 75%, bandwidth usage

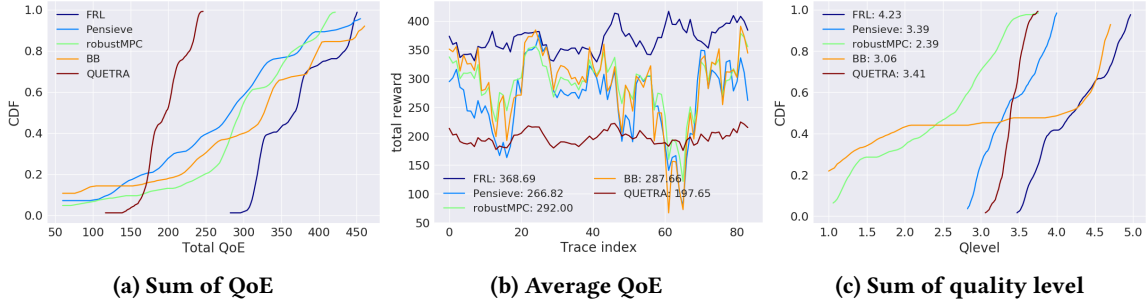


Figure 7: QoE performance.

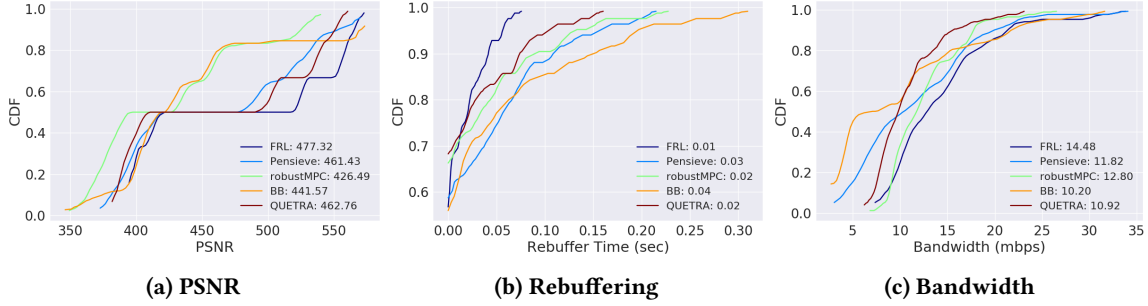


Figure 8: Key metrics performance.

by 32%, 22%, 13%, and 42%, compared to QUETRA, Pensieve, robustMPC, and BB, respectively.

Note that we have overall 5 encoding quality levels (each level has a compressed and uncompressed version), therefore the improvements over baselines can be approximately seen as improving the average quality by 1, 1, 4, and 2 levels, which aligns with the improvement results of PSNR. For the same reason, FRL presents higher bandwidth usage than the baselines. However, FRL presents the minimal rebuffering out of all tested algorithms, which indicates FRL causes the lowest frequency of bandwidth saturation. Hence, it shows that FRL can best utilizes the available bandwidth to achieve the best performance trade-off and QoE.

Demo. We ran real-world tests for all the algorithms on the prototype system with point cloud videos in real wireless networks. Figure 9 shows a sequence of point cloud video frames sampled approximately every two seconds. FRAS shows the best frame quality out of all the streaming algorithms, which validate the superiority of FRL and practicability of FRAS.

6 CONCLUSION

Point cloud streaming plays a key role in multimedia especially for volumetric videos. Its unique features such as 6DoF and decoding complexity demands innovative QoE definition and ABR algorithms. In this work, we propose FRAS, the first federated reinforcement learning framework, to the best of

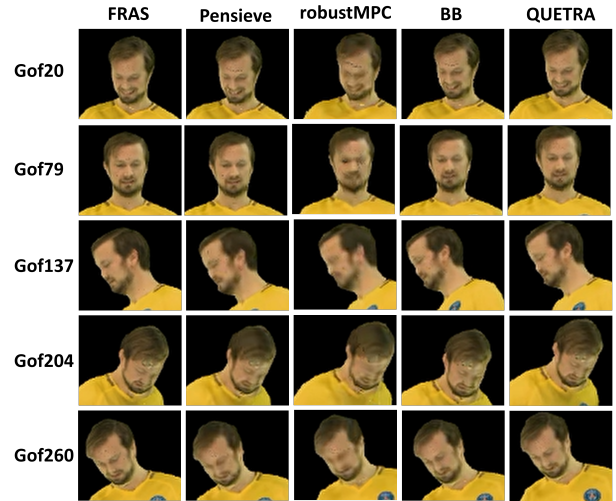


Figure 9: Demo results (zoom in for better observation).

our knowledge, for adaptive point cloud video streaming. FRAS is an end-to-end framework which takes the unique features of point cloud into account and augment learning performance by aggregating distributed modes of users but with privacy preservation. Empirical evaluations and prototype demo have shown the superior performance of FRAS in numerous perspectives.

REFERENCES

- [1] Zahaib Akhtar, Yun Seong Nam, Ramesh Govindan, Sanjay Rao, Jessica Chen, Ethan Katz-Basnett, Bruno Ribeiro, Jibin Zhan, and Hui Zhang. 2018. Oboe: auto-tuning video ABR algorithms to network conditions. In *SIGCOMM*.
- [2] Evangelos Alexiou, Evgeniy Upenik, and Touradj Ebrahimi. 2017. Towards subjective quality assessment of point cloud imaging in augmented reality. In *2017 IEEE 19th International Workshop on Multimedia Signal Processing (MMSp)*. IEEE, 1–6.
- [3] Chao Cao, Marius Preda, and Titus Zaharia. 2019. 3D Point Cloud Compression: A Survey. In *The 24th International Conference on 3D Web Technology*. ACM, 1–9.
- [4] Maxim Claeys, Steven Latre, Jeroen Famaey, and Filip De Turck. 2014. Design and evaluation of a self-learning HTTP adaptive video streaming client. *IEEE communications letters* 18, 4 (2014), 716–719.
- [5] Alexander Clemm, Maria Torres Vega, Hemanth Kumar Ravuri, Tim Wauters, and Filip De Turck. 2020. Toward Truly Immersive Holographic-Type Communication: Challenges and Solutions. *IEEE Communications Magazine* 58, 1 (2020), 93–99.
- [6] E d'Eon, Bob Harrison, T Myers, and PA Chou. 2017. 8i voxelized full bodies-a voxelized point cloud dataset. *ISO/IEC JTC1/SC29 Joint WG11/WG1 (MPEG/JPEG) input document WG11M40059/WG1M74006*, Geneva (2017).
- [7] Rui Fu, Zuo Zhang, and Li Li. 2016. Using LSTM and GRU neural network methods for traffic flow prediction. In *2016 31st Youth Academic Annual Conference of Chinese Association of Automation (YAC)*. IEEE, 324–328.
- [8] Chengjun Guo, Ying Cui, and Zhi Liu. 2018. Optimal Multicast of Tiled 360 VR Video in OFDMA Systems. *IEEE Communications Letters* 22, 12 (2018), 2563–2566.
- [9] Mohammad Hosseini and Christian Timmerer. 2018. Dynamic adaptive point cloud streaming. In *Proceedings of the 23rd Packet Video Workshop*. ACM, 25–30.
- [10] Xueshi Hou, Jianzhong Zhang, Madhukar Budagavi, and Sujit Dey. 2019. Head and Body Motion Prediction to Enable Mobile VR Experiences with Low Latency. In *2019 IEEE Global Communications Conference (GLOBECOM)*. IEEE, 1–7.
- [11] Te-Yuan Huang, Ramesh Johari, Nick McKeown, Matthew Trunnell, and Mark Watson. 2014. A buffer-based approach to rate adaptation: Evidence from a large video streaming service. In *Proceedings of the 2014 ACM conference on SIGCOMM*. 187–198.
- [12] Peter Kairouz, H Brendan McMahan, Brendan Avent, Aurélien Bellet, Mehdi Bennis, Arjun Nitin Bhagoji, Keith Bonawitz, Zachary Charles, Graham Cormode, Rachel Cummings, et al. 2019. Advances and open problems in federated learning. *arXiv preprint arXiv:1912.04977* (2019).
- [13] Jie Li, Cong Zhang, Zhi Liu, Wei Sun, and Qiyue Li. 2020. Joint Communication and Computational Resource Allocation for QoE-driven Point Cloud Video Streaming. *IEEE International Conference on Communications (ICC)* (2020).
- [14] Zhi Liu, Jie Li, Xianfu Chen, Celimuge Wu, Susumu Ishihara, and Yusheng Ji. 2020. Fuzzy Logic-Based Adaptive Point Cloud Video Streaming. *IEEE Open Journal of the Computer Society* 1 (2020), 121–130.
- [15] Zhi Liu, Qiyue Li, Xianfu Chen, Celimuge Wu, Susumu Ishihara, Jie Li, and Yusheng Ji. 2021. Point Cloud Video Streaming: Challenges and Solutions. *IEEE Network* 35, 5 (2021), 202–209.
- [16] Hongzi Mao, Ravi Netravali, and Mohammad Alizadeh. 2017. Neural adaptive video streaming with pensieve. In *Proceedings of the Conference of the ACM Special Interest Group on Data Communication*. 197–210.
- [17] Brendan McMahan, Eider Moore, Daniel Ramage, Seth Hampson, and Blaise Agüera y Arcas. 2017. Communication-efficient learning of deep networks from decentralized data. In *Artificial intelligence and statistics*. PMLR, 1273–1282.
- [18] Rufael Mekuria, Kees Blom, and Pablo Cesar. 2016. Design, implementation, and evaluation of a point cloud codec for tele-immersive video. *IEEE Transactions on Circuits and Systems for Video Technology* 27, 4 (2016), 828–842.
- [19] Volodymyr Mnih, Adria Puigdomenech Badia, Mehdi Mirza, Alex Graves, Timothy Lillicrap, Tim Harley, David Silver, and Koray Kavukcuoglu. 2016. Asynchronous methods for deep reinforcement learning. In *International conference on machine learning*. PMLR, 1928–1937.
- [20] Jounsup Park, Philip A Chou, and Jenq-Neng Hwang. 2019. Rate-utility optimized streaming of volumetric media for augmented reality. *IEEE Journal on Emerging and Selected Topics in Circuits and Systems* 9, 1 (2019), 149–162.
- [21] Feng Qian, Bo Han, Jarrell Pair, and Vijay Gopalakrishnan. 2019. Toward Practical Volumetric Video Streaming on Commodity Smartphones. In *Proceedings of the 20th International Workshop on Mobile Computing Systems and Applications*. ACM, 135–140.
- [22] Sebastian Schwarz, Marius Preda, Vittorio Baroncini, Madhukar Budagavi, Pablo Cesar, Philip A Chou, Robert A Cohen, Maja Krivokuća, Sébastien Lasserre, Zhu Li, et al. 2018. Emerging MPEG standards for point cloud compression. *IEEE Journal on Emerging and Selected Topics in Circuits and Systems* 9, 1 (2018), 133–148.
- [23] J. van der Hooft, S. Petrangeli, T. Wauters, R. Huysegems, P. R. Alfance, T. Bostoen, and F. De Turck. 2016. HTTP/2-Based Adaptive Streaming of HEVC Video Over 4G/LTE Networks. *IEEE Communications Letters* 20, 11 (2016), 2177–2180.
- [24] Jeroen van der Hooft, Tim Wauters, Filip De Turck, Christian Timmerer, and Hermann Hellwagner. 2019. Towards 6dof http adaptive streaming through point cloud compression. In *Proceedings of the 27th ACM International Conference on Multimedia*. 2405–2413.
- [25] Andrew D Wilson. 2017. Fast lossless depth image compression. In *Proceedings of the 2017 ACM International Conference on Interactive Surfaces and Spaces*. 100–105.
- [26] Yuhuai Wu, Elman Mansimov, Roger B Grosse, Shun Liao, and Jimmy Ba. 2017. Scalable trust-region method for deep reinforcement learning using kronecker-factored approximation. *Advances in neural information processing systems* 30 (2017).
- [27] Wenqian Xue, Jialu Fan, Victor G Lopez, Jinna Li, Yi Jiang, Tianyou Chai, and Frank L Lewis. 2019. New methods for optimal operational control of industrial processes using reinforcement learning on two time-scales. *IEEE Transactions on Industrial Informatics* (2019).
- [28] Praveen Kumar Yadav, Arash Shafiei, and Wei Tsang Ooi. 2017. Quetra: A queuing theory approach to dash rate adaptation. In *Proceedings of the 25th ACM international conference on Multimedia*. 1130–1138.
- [29] Hyunho Yeo, Youngmok Jung, Jaehong Kim, Jinwoo Shin, and Dongsu Han. 2018. Neural adaptive content-aware internet video delivery. In *OSDI*.
- [30] Xiaoqi Yin, Abhishek Jindal, Vyas Sekar, and Bruno Sinopoli. 2015. A control-theoretic approach for dynamic adaptive video streaming over HTTP. In *Proceedings of the 2015 ACM Conference on Special Interest Group on Data Communication*. 325–338.
- [31] Michael Zink, Ramesh Sitaraman, and Klara Nahrstedt. 2019. Scalable 360° Video Stream Delivery: Challenges, Solutions, and Opportunities. *Proc. IEEE* (2019).